

## 11.6 A Temperature-to-Digital Converter for a MEMS-Based Programmable Oscillator with Better Than $\pm 0.5$ ppm Frequency Stability

Michael Perrott<sup>1</sup>, Jim Salvia<sup>2</sup>, Fred Lee<sup>3</sup>, Aaron Partridge<sup>2</sup>, Shouvik Mukherjee<sup>2</sup>, Carl Arft<sup>2</sup>, Jin-Tae Kim<sup>2</sup>, Niveditha Arumugam<sup>2</sup>, Pavan Gupta<sup>2</sup>, Sassan Tabatabaei<sup>2</sup>, Sudhakar Pamarti<sup>4</sup>, Haechang Lee<sup>2</sup>, Fari Assaderaghi<sup>2</sup>

<sup>1</sup>Masdar Institute of Science and Technology, Abu Dhabi, United Arab Emirates,

<sup>2</sup>SiTime, Sunnyvale, CA

<sup>3</sup>Fairchild Semiconductor, San Jose, CA

<sup>4</sup>University of California, Los Angeles, Los Angeles, CA

MEMS-based programmable oscillators have emerged as a promising alternative to crystal-based frequency references, with previously reported work demonstrating sub-ps integrated jitter [1]. Here we show frequency stability better than  $\pm 0.5$ ppm from  $-40$  to  $85^\circ\text{C}$ , along with Allan Deviation (i.e., long term jitter) better than  $0.005$  ppm for  $0.1$ ,  $1$ , and  $10$  second strides. Since the MEMS resonator has a well-defined temperature dependence, the key to this performance is a stable and low-noise temperature-to-digital converter (TDC) that utilizes a thermistor on the same die as the MEMS resonator.

Figure 11.6.1 illustrates our programmable oscillator. It consists of a MEMS resonator die which is wire bonded to a  $0.18\mu\text{m}$  CMOS die that includes an oscillator sustaining circuit, TDC, fractional-N synthesizer, and digital logic [1]. Placement of a thermistor on the MEMS die allows excellent tracking of temperature-induced fluctuations of the MEMS resonator frequency,  $F_{\text{res}}$ . Compensation of nonlinear temperature dependence of the thermistor resistance and  $F_{\text{res}}$  is achieved with on-chip digital 5<sup>th</sup>-order polynomial correction. Since  $F_{\text{res}}$  varies by approximately  $-31$ ppm/K, it is challenging to obtain  $\pm 0.5$ ppm frequency stability from  $-40$  to  $85^\circ\text{C}$ . The current state of the art is  $\pm 10$ ppm frequency stability for temperature compensated (non-ovenized) MEMS oscillators [4]. Further, noise lower than  $0.16$ mK (rms) in a  $5$ Hz bandwidth (i.e.,  $10$ S/s) is required to achieve Allan Deviation less than  $0.005$ ppm at  $0.1$  second stride – a challenging requirement given the current state of the art of  $2$ mK at  $1$ S/s [2],  $15$ mK at  $10$  S/s [3] and  $40$ mK at  $32$  S/s [4].

The TDC's front-end circuit, shown in Fig. 11.6.2, consists of a resistive bridge that is balanced by digitally tuning a reference resistor,  $R_{\text{ref}}$ , to match the thermistor's resistance,  $R_{\text{MEMS}}$ . Comparison of  $R_{\text{ref}}$  and  $R_{\text{MEMS}}$  is achieved by using a CMOS switch to periodically short them together at frequency  $f_{\text{chop}}$  ( $25$ kHz), and then amplifying the sum of the two voltages,  $V_R(t)$  and  $V_C(t)$ , to yield an output voltage,  $V_{\text{amp}}(t)$ . As shown in Fig. 11.6.2,  $V_R(t)$  and  $V_C(t)$  move in opposite directions, and, regardless of the small resistance of the shorting switch, will have equal changes in magnitude only when  $R_{\text{ref}}$  and  $R_{\text{MEMS}}$  are equal in value (assuming well matched  $C_{\text{ac}}$  capacitors). As such, sampling the change in  $V_{\text{amp}}(t)$  between each phase of  $f_{\text{chop}}$ ,  $V_{\text{avg1}}[\text{k}] - V_{\text{avg2}}[\text{k}]$ , provides an accurate error signal for tuning  $R_{\text{ref}}$  to match  $R_{\text{MEMS}}$ . An advantage of this CDS technique is that it rejects the  $1/f$  noise and DC offset of the front-end amplifier. Further, the amplifier's DC input biasing can be done in an essentially noise free manner via a feedback resistor,  $R_f$ , which is periodically switched into the circuit for brief intervals outside the measurement window of  $V_{\text{avg1}}[\text{k}]$  and  $V_{\text{avg2}}[\text{k}]$ .

Figure 11.6.3 reveals that  $R_{\text{ref}} = T_{\text{clk}}/C_2$  is implemented with a switched-capacitor (SC) network, where  $f_{\text{clk}} = 1/T_{\text{clk}}$  is the frequency, in the tens of MHz range, of the non-overlapping clocks  $\text{clk}_{\text{ph1}}(t)$  and  $\text{clk}_{\text{ph2}}(t)$ . By digitally varying  $f_{\text{clk}}$ , the SC reference resistor can be tuned with high resolution. Voltage ripple due to the SC operation is reduced by the  $C_1$  capacitors. Pseudo-differential implementation of the front-end is achieved with only one thermistor by using additional switches controlled by  $\text{clk}_{\text{chop}}(t)$ , which suppresses electromigration-induced drift since DC current through the thermistor is nearly zero.

Similar to the pulsed resistor biasing shown in Fig. 11.6.2, Fig. 11.6.3 reveals that a simple voltage regulator to reduce supply noise is achieved for the amplifier by pulse biasing the gate of a native NMOS device. A similar technique is also applied to the current bias source, with  $R_{\text{bias}}$  reducing the impact of charge injection and  $C_{\text{bias}}$  being large enough to adequately maintain the voltage bias

between pulses. The measurement windows of  $V_{\text{amp,p}}(t)$  and  $V_{\text{amp,m}}(t)$  are chosen to avoid the intervals during which pulsed biasing occurs as well as the transients due to the transitions of  $\text{clk}_{\text{chop}}(t)$ .

A system-level view of the TDC is shown in Fig. 11.6.4.  $R_{\text{ref}} = T_{\text{clk}}/C_2$  is digitally tuned using a fractional-N frequency divider whose nominal divide value,  $N_{\text{nom}}$ , is set by a 2<sup>nd</sup>-order digital  $\Delta\Sigma$  modulator such that  $R_{\text{ref}} = T_{\text{clk480}} \cdot N_{\text{nom}}/C_2$ .  $T_{\text{clk480}}$  is set by an on-chip ring-oscillator clock multiplier that creates a  $480$ MHz clock signal locked to the  $F_{\text{res}}$  frequency ( $48$ MHz).  $N_{\text{nom}}$  is adjusted by the feedback loop to achieve  $V_{\text{avg1}}[\text{k}] - V_{\text{avg2}}[\text{k}] = 0$ , implying  $R_{\text{ref}} = R_{\text{MEMS}}$  under steady-state conditions. The overall TDC output at steady-state is  $N_{\text{nom}} = R_{\text{MEMS}} \cdot C_2/T_{\text{clk480}}$ . Since 5<sup>th</sup>-order polynomial correction is employed, temperature-induced variations in  $C_2$  (implemented as a metal finger capacitor) and  $T_{\text{clk480}}$  (derived from  $F_{\text{res}}$ ) are acceptable since they do not introduce significant higher-order curvature or cancellation of the temperature-induced variation in  $R_{\text{MEMS}}$ .

Details of the VCO-based quantizer are shown in Fig. 11.6.5. A pseudo-differential implementation is utilized [5,6] in which two ring oscillators are shifted in opposite directions in frequency as a function of the differential input voltage,  $V_{\text{in+}} - V_{\text{in-}}$ . The oscillators' biasing network keeps their total current consumption relatively constant in order to reduce impact on the supply voltage, and small bleeder currents maintain oscillation above  $150$ MHz. In order to sample the phase of the ring oscillator outputs at a relatively low rate of  $24$ MHz,  $6$ b digital counters are inserted between the ring oscillators and the sampling register. The sampling register also includes digital logic to compensate for wrapping effects on the digital counters, and the 1<sup>st</sup>-order difference transforms the sampled phase of each oscillator into the difference of their frequencies while yielding 1<sup>st</sup>-order shaped quantization noise. Implementation of the measurement windows of  $V_{\text{avg1}}[\text{k}]$  and  $V_{\text{avg2}}[\text{k}]$  is achieved by the digital averaging block, which simply ignores the output of the VCO-based quantizer outside these measurement windows.

Figure 11.6.7 shows a die photo of the MEMS resonator die (with thermistor) wire-bonded to the  $0.18\mu\text{m}$  CMOS die. Overall measured chip current ( $48$ MHz output with no load) is  $33$ mA at  $3.3$ V supply. Measured current consumption for the combined TDC and clock multiplier (including all analog and digital circuits) is  $3.93$ mA, of which  $2.8$ mA is estimated for the analog portion of the TDC and entire clock multiplier (which occupy  $0.18$ mm<sup>2</sup> combined area), and the remainder for digital blocks. TDC noise in  $5$ Hz bandwidth is  $<100\mu\text{K}$  (rms) at  $25^\circ\text{C}$  based on measurements taken from the TDC output. Figure 11.6.6(a) shows better than  $\pm 0.5$ ppm stability from  $-40$  to  $85^\circ\text{C}$  with frequency compensation consisting solely of the on-chip TDC and digital 5<sup>th</sup>-order polynomial correction. Figure 11.6.6(b) displays measured output phase noise under several different conditions related to the TDC. Finally, Fig. 11.6.6(c) shows measured Allan Deviation  $<0.005$ ppm at room temperature at  $0.1$ ,  $1$ , and  $10$ -second strides.

### Acknowledgements:

Renata Melamud, Paul Hagelin, and Charles Grosjean developed the MEMS resonator. Bruno Garlepp and Cathy Lee made important circuit contributions. Kofi Makinwa provided many valuable comments for this paper.

### References:

- [1] F.S. Lee, J. Salvia, C. Lee, *et al.*, "A Programmable MEMS-Based Clock Generator with Sub-ps Jitter Performance", *VLSI Circuits Symp.*, pp. 158-159, June 2011.
- [2] M. Pertijs, K.A.A. Makinwa, and J.H. Huijsing, "A CMOS Smart Temp. Sensor With a  $3\sigma$  Inaccuracy of  $0.1^\circ\text{C}$  From  $55^\circ\text{C}$  to  $125^\circ\text{C}$ ," *IEEE J. Solid-State Circuits*, vol. 40, no. 12, pp. 2805-2815, Dec. 2005.
- [3] K. Souri and K.A.A. Makinwa, "A  $0.12\text{mm}^2$   $7.4\mu\text{W}$  Micropower Temp. Sensor with an Inaccuracy of  $0.2^\circ\text{C}$  ( $3\sigma$ ) from  $-30^\circ\text{C}$  to  $125^\circ\text{C}$ ," *IEEE J. Solid-State Circuits*, vol. 46, no. 7, pp. 1693-1700, July 2011.
- [4] D. Ruffieux, F. Krummenacher, A. Pezous, and G. Spinola-Durante, "Silicon Res. Based  $3.2\mu\text{W}$  Real Time Clock With  $10$ ppm Freq. Accuracy," *IEEE J. Solid-State Circuits*, vol. 45, no. 1, pp. 224-234, Jan. 2010.
- [5] U. Wismar, D. Wisland, and P. Andreani, "A  $0.2$  V,  $7.5\mu\text{W}$ ,  $20$ kHz  $\Sigma\Delta$  modulator with  $69$  dB SNR in  $90$  nm CMOS," *Proc. ESSCIRC*, pp. 206-209, Sept. 2007.
- [6] G. Taylor and I. Galton, "A Mostly-Digital Variable-Rate Continuous-Time Delta-Sigma Modulator ADC," *IEEE J. Solid-State Circuits*, vol. 45, no. 12, pp. 2634-2646, Dec. 2010.

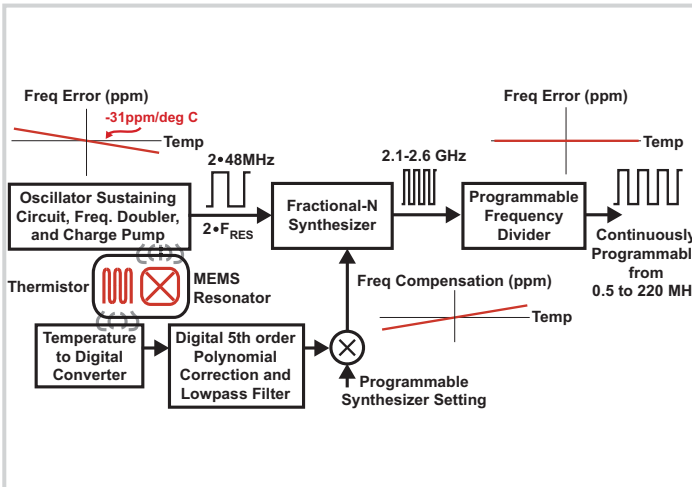


Figure 11.6.1: MEMS-based oscillator circuit consisting of a MEMS die with resonator and thermistor wire-bonded to a CMOS die with sustaining circuit, frequency doubler, fractional-N synthesizer, programmable frequency divider, and temperature compensation circuits.

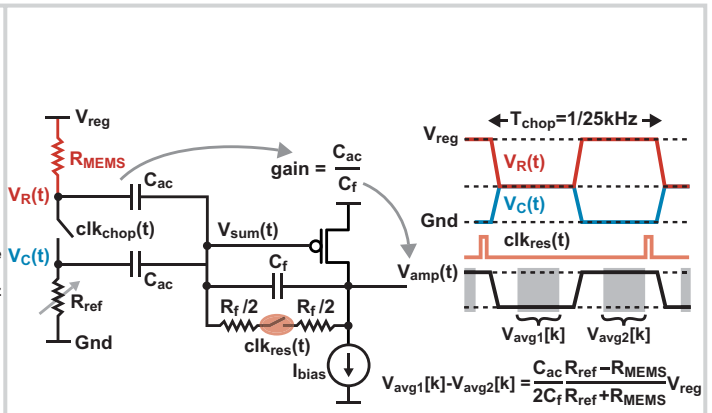


Figure 11.6.2: Simplified view of TDC frontend in which  $R_{ref}$  is matched to  $R_{MEMS}$  with error sensed using an amplifier with pulsed resistor feedback biasing for reduced noise.

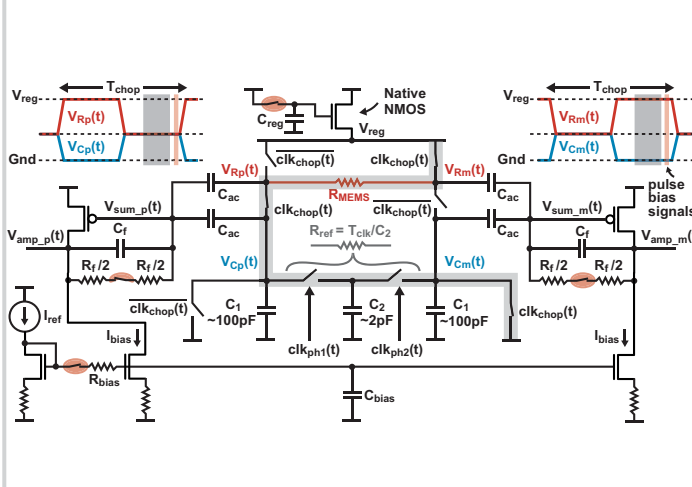


Figure 11.6.3: Detailed view of pseudo-differential TDC frontend showing the switched-capacitor implementation of  $R_{ref}$  and the pulsed bias current mirror and voltage regulator for reduced noise.

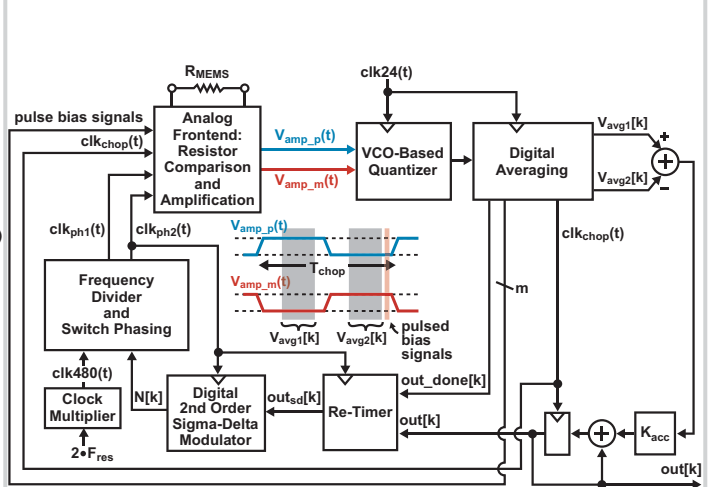


Figure 11.6.4: System-level view of TDC.

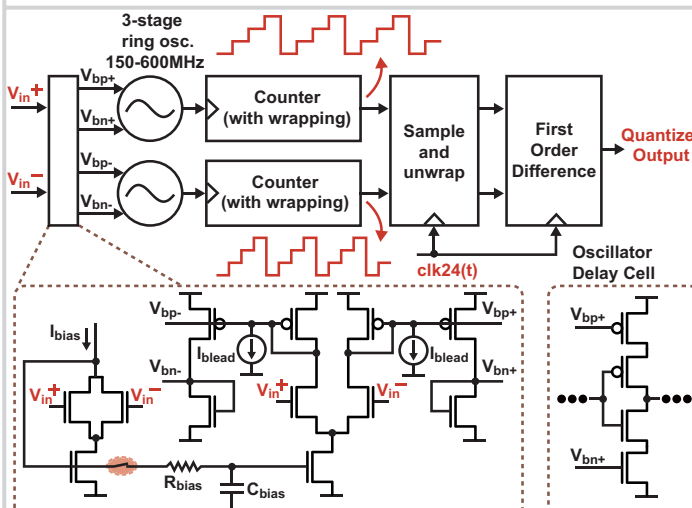


Figure 11.6.5: Pseudo-differential VCO-based quantizer in which counters are leveraged to lower the required sampling rate of the quantizer and pulsed current biasing for reduced noise.

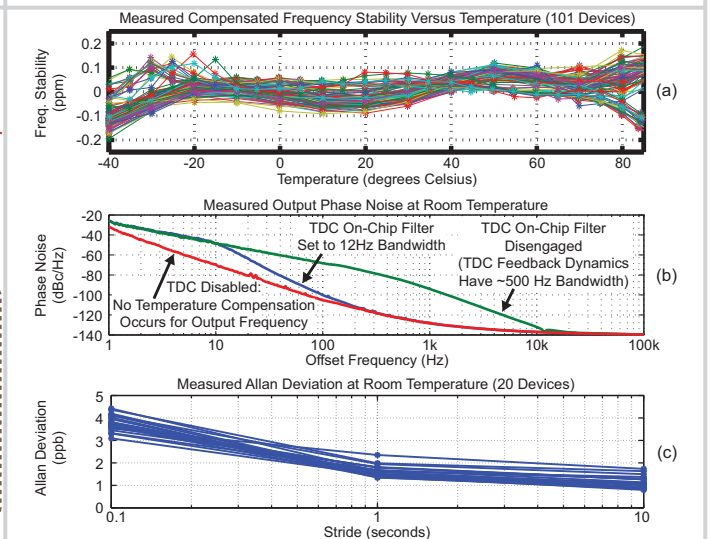


Figure 11.6.6: Measured results for (a) compensated frequency stability, (b) output phase noise at several TDC settings, and (c) Allan Deviation.

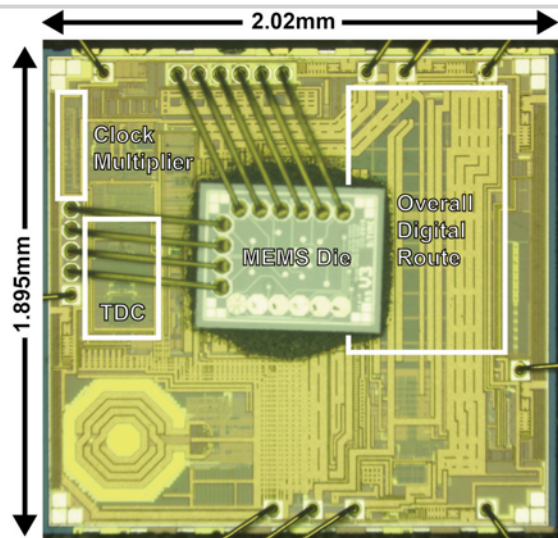


Figure 11.6.7: Micrograph of the 0.18 $\mu\text{m}$  CMOS die with MEMS die of the resonator and thermistor attached on top.